Cell Reports
Article

Facilitates Chromatin Transcription Complex Is an "Accelerator" of Tumor Transformation and Potential Marker and Target of Aggressive Cancers

Henry Garcia,[1] Jeffrey C. Miecznikowski,[2] Alfiya Safina,[1] Mairead Commane,[1] Anja Ruusulehto,[3] Sami Kilpinen,[3] Robert W. Leach,[4] Kristopher Attwood,[5] Yan Li,[5] Seamus Degan,[1] Angela R. Omilian,[6] Olga Guryanova,[7] Olympia Papantonopoulou,[1] Jianmin Wang,[5] Michael Buck,[8] Song Liu,[5] Carl Morrison,[6,*] and Katerina V. Gurova[1,*]
[1]Department of Cell Stress Biology, Roswell Park Cancer Institute, Elm and Carlton Streets, Buffalo, NY 14263, USA
[2]Department of Biostatistics, SUNY Buffalo, Buffalo, NY 14263, USA
[3]MediSapiens, Ltd., Tukholmankatu 8 A, 00290 Helsinki, Finland
[4]Center for Computational Research, SUNY Buffalo, Buffalo, NY 14263, USA
[5]Department of Biostatistics and Bioinformatics, Roswell Park Cancer Institute, Elm and Carlton Streets, Buffalo, NY 14263, USA
[6]Department of Pathology, Roswell Park Cancer Institute, Elm and Carlton Streets, Buffalo, NY 14263, USA
[7]Human Oncology and Pathogenesis Program, Memorial Sloan-Kettering Cancer Center, New York, NY 10065, USA
[8]Department of Biochemistry, SUNY Buffalo, Buffalo, NY 14263, USA
*Correspondence: carl.morrison@roswellpark.org (C.M.), katerina.gurova@roswellpark.org (K.V.G.)
http://dx.doi.org/10.1016/j.celrep.2013.06.013

SUMMARY

The facilitates chromatin transcription (FACT) complex is involved in chromatin remodeling during transcription, replication, and DNA repair. FACT was previously considered to be ubiquitously expressed and not associated with any disease. However, we discovered that FACT is the target of a class of anticancer compounds and is not expressed in normal cells of adult mammalian tissues, except for undifferentiated and stem-like cells. Here, we show that FACT expression is strongly associated with poorly differentiated aggressive cancers with low overall survival. In addition, FACT was found to be upregulated during in vitro transformation and to be necessary, but not sufficient, for driving transformation. FACT also promoted survival and growth of established tumor cells. Genome-wide mapping of chromatin-bound FACT indicated that FACT's role in cancer most likely involves selective chromatin remodeling of genes that stimulate proliferation, inhibit cell death and differentiation, and regulate cellular stress responses.

INTRODUCTION

The facilitates chromatin transcription (FACT) complex is a heterodimer of two subunits: Structure-Specific Recognition Protein 1 (SSRP1) and Suppressor of Ty (SPT16). FACT plays a role in chromatin remodeling by modulating nucleosome stability (Reinberg and Sims, 2006; Singer and Johnston, 2004) and has been implicated in multiple processes involving chromatin, including transcription and DNA replication, recombination, and repair (Saunders et al., 2003; Belotserkovskaya et al., 2003; Birch et al., 2009; Tan et al., 2006, 2010; Zhou and Wang, 2004; Kumari et al., 2009; Heo et al., 2008; Keller et al., 2001; Ikeda et al., 2011). Our recent discovery that FACT is the molecular target of a class of anticancer compounds, Curaxins (CXs), provided indication that FACT might play a role in cancer (Gasparian et al., 2011). This possibility is supported by our findings that FACT is expressed at higher levels in tumor cell lines than in normal cells in vitro and that RNAi-mediated knockdown (KD) of FACT expression leads to reduced growth and survival of tumor cells (Gasparian et al., 2011). In addition, FACT expression was found to be elevated during the development of mammary carcinomas in transgenic mice expressing the *Her2/neu* proto-oncogene (Koman et al., 2012). FACT's pattern of expression in normal (nontumor) cells is also consistent with a possible role in tumorigenesis. Although FACT was previously considered a ubiquitously expressed housekeeping factor (reviewed in Singer and Johnston, 2004), we did not detect SSRP1 or SPT16 expression in normal organs of adult humans or mice, with the exception of some cell types in hematological and reproductive organs and intestinal crypts (Garcia et al., 2011). Analysis of publicly available gene expression data from multiple studies revealed that FACT is expressed at high levels in undifferentiated stem and progenitor cells in different organs and that its expression decreases upon differentiation (Garcia et al., 2011).

Herein, we confirmed the association between FACT and cancer by showing that FACT expression increases during in vitro transformation of normal cells and is functionally required for transformation as well as tumor cell survival and growth. We showed that FACT is frequently expressed in different types of tumors and established a statistically significant association between the frequency and level of SSRP1 and tumor aggressiveness. To address the mechanism(s) by which FACT

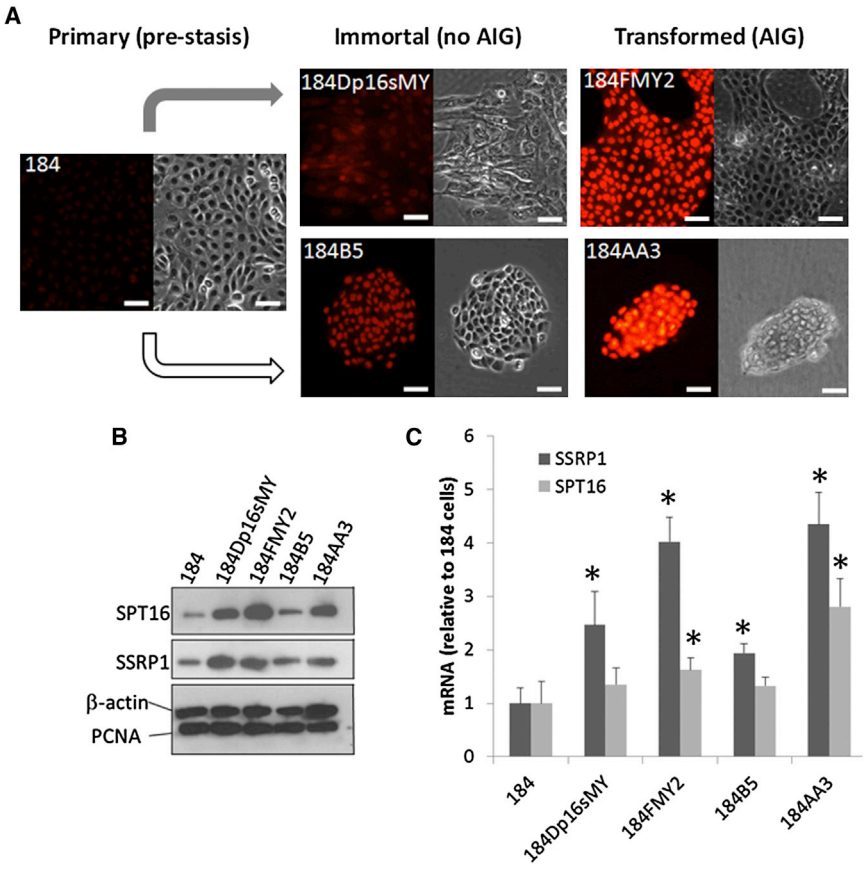

Figure 1. FACT Subunit Levels Are Elevated in the Process of In Vitro Transformation

(A–C) HMECs were transformed using genetic (gray arrow) or chemical (white arrow) manipulations. Primary (184), immortal (184Dp16sMY, 184B5), and fully transformed (184FMY2, 184AA3) cells were assessed by (A) immunofluorescent staining with antibodies to SSRP1 (scale bars, 100 μM); (B) western blotting with the indicated antibodies; and (C) quantitative reverse-transcription PCR analysis of total RNA with primers specific to *SSRP1*, or *SPT16* or *18S* rRNA (loading control). Data in (C) were normalized based on the level of *18S* rRNA and are shown relative to the level of the corresponding transcripts in 184 cells (set at 1.0). Bars indicate the mean of three replicates + SD. *$p < 0.05$ for comparison to 184 cells. See also Figure S1.

facilitates tumor growth, we assessed genome-wide distribution of FACT binding to chromatin in tumor cells. This identified a subset of genes that are likely dependent upon FACT for expression and that have activities associated with malignant and stem-like properties of tumor cells and cellular stress responses.

RESULTS

FACT Is Elevated during In Vitro Transformation

To test the hypothesis that FACT plays a role in tumorigenesis, we compared SSRP1 and SPT16 protein levels in cultured cells of mesenchymal or epithelial origin representing different stages of (in vitro) transformation: finite lifespan, immortalized, or transformed. There was essentially no change in FACT levels between normal human fibroblasts and fibroblasts immortalized with human telomerase or between mouse primary fibroblasts from *p53* wild-type (finite) or knockout (immortalized) animals (Figure S1A). However, when we transformed immortalized fibroblasts of either human or mouse origin with activated *H-Ras*^{V12} oncogene, we observed a dramatic increase in FACT levels (Figures S1B and S1C). Importantly, the fibroblasts (finite lifespan, immortalized, or transformed) did not have significantly different proliferation rates; therefore, FACT upregulation was not a reflection of increased cell proliferation.

To model epithelial cell transformation, we used previously described human mammary epithelial cell (HMEC) strains from breast reduction specimens (Garbe et al., 2009) and isogenic immortalized and transformed lines derived from these cells via exposure to the chemical carcinogen benzo(a)pyrene (Stampfer and Bartley, 1985) or expression of shRNA against *CDKN2A* (p16) and/or the cDNA of proto-oncogene *c-MYC* (Brenner et al., 1998), respectively (Figure 1). The parental (normal) HMEC strains (184) showed almost no nuclear SSRP1 staining, whereas transformed derivatives capable of anchorage-independent growth (AIG) (184FMY2 and 184AA3) were strongly SSRP1 positive (Figure 1A). Immortalized lines not capable of AIG displayed weak but detectable SSRP1 staining. Increased SSRP1 and SPT16 expression in successive stages of in vitro transformation was confirmed by both western blotting (Figure 1B) and quantitative reverse-transcription PCR (Figure 1C). Analysis of PCNA protein expression showed that these differences were not due to differences in proliferation (Figure 1B).

FACT Expression Is Required for Transformation and for Tumor Cell Survival and Growth

To determine the functional importance of FACT elevation during transformation, we evaluated how changes in FACT levels affected the efficiency of *H-Ras*^{V12}-induced transformation of fibroblasts and epithelial cells. We transduced *p53*$^{-/-}$ mouse embryonic fibroblast (MEF) or MCF10A (immortalized nontransformed HMEC) with lentiviral *H-Ras*^{V12} together with either expression constructs for both FACT subunits or shRNAs targeting them. In both cell types, the efficiency of transformation was increased by enforced FACT expression and decreased by FACT KD. However, there were some cell-type-specific differences. Although MEFs proliferated equally well in 2D culture with or without elevated FACT, growth of epithelial MCF10A cells was induced by FACT overexpression (Figure 2A, compare "Empty vectors" with "SSRP1+SPT16" panels). Moreover, transduction of MCF10A cells with *H-Ras* ^{V12} led to the massive

appearance of enlarged flat vacuolated senescent-like cells and a minor population of small, growing, transformed-looking cells that became the majority after replating (Figure 2A, "H-Ras^{V12}" plus "Empty vectors" panel). Overexpression of FACT together with *H-Ras* ^{V12} significantly increased the proportion of actively growing transformed-like cells, which quickly became predominant even without passaging (Figure 2A, "H-Ras^{V12}" plus "SSRP1+SPT16" panel). Transduction of *H-Ras*^{V12} into fibroblast and epithelial cells leads to the appearance of cells able to grow in semisolid medium and in vivo in animals. FACT overexpression significantly increased the proportion of these cells (Figures S1D, S1E, and 2B), whereas FACT KD almost completely eliminated them (Figures 2C and 2D). Importantly, overexpression of FACT alone (without *H-Ras* ^{V12}) was not sufficient to induce MEF or MCF10A cells to grow in semisolid media (Figures S1D, S1E, and 2B). These data suggest that FACT promotes, but cannot on its own drive, cellular transformation.

To test if FACT is also essential for established transformed cells, we compared the effects of FACT KD on the growth of pairs of tumor and nontransformed "normal" cells of the same tissue (fibroblasts, kidney and mammary epithelia; Figure 2E). It should be noted that unlike primary normal cells in vitro or in vivo, all tested established cell lines (transformed and nontransformed) express both FACT subunits (Figure 2F). Because a parallel study demonstrated coregulation of SSRP1 and SPT16 levels, shRNA against either FACT subunit effectively eliminated both SSRP1 and SPT16 (Safina et al., 2013). We found that FACT KD suppressed the growth of all tumor cells but had a smaller or no effect on the growth of nontransformed cells (Figure 2E). For two out of three cell pairs (kidney and fibroblasts cells), nontransformed cells surviving shRNA transduction showed effective FACT KD, whereas corresponding tumor cells did not (Figure 2F). These data suggested that unlike nontransformed cells, tumor cells cannot grow in the absence of FACT. This was subsequently confirmed in the MCF7 (tumor)/MCF10A (nontumor) cell pair through comparison of cell growth and FACT expression at different times after transduction of shSSRP1 or shSPT16 (Figure S2).

Further illustrating that FACT is required for tumor cell growth, immunofluorescent staining of shSSRP1-transduced cell cultures revealed that the proportion of cells with low SSRP1 levels decreases with time (Figure 2G). Moreover, tumor cells with low FACT levels had reduced replication rates (Figures 2H and 2I) accumulated in G1 (Figure 2H), and some died (Figure 2H, red arrow, and Figure 2J). Although these data support a role for FACT in DNA replication, the absence of S phase arrest (which would be expected if FACT is needed only for replication) suggests that signaling leading to G1 arrest and/or other FACT-dependent processes (e.g., transcription) may also be vital for tumor cells.

Chromatin-Embedded FACT Is Enriched at Genes Associated with Cancer and Cell Pluripotency

The known activities of FACT suggest that it may promote tumor growth by altering chromatin in a way that facilitates transcription of genes important for transformation. FACT does not affect general transcription (Figures S3A–S3C) but has been shown to be required for transcription driven by particular transcription factors (TFs) such as NF-κB (Gasparian et al., 2011), the activity of which is critical for many types of tumor cells (Gudkov et al., 2011). To identify other FACT-dependent transcriptional programs or genes, we used chromatin immunoprecipitation (ChIP) followed by next-generation sequencing (NGS) to examine the distribution of chromatin-bound FACT in HT1080 tumor cells, the growth and survival of which require FACT (Figures 2E–2J). Three independent ChIP experiments were performed on unsynchronized, growing HT1080 with anti-SSRP1 antibodies shown to be highly specific (LC/MS of immunoprecipitated complex) and not interfere with either SSRP1/SPT16 association or binding of FACT to chromatin (Figure S4; Gasparian et al., 2011). As a specificity control for anti-SSRP1 ChIP, we used cells treated with the small molecule CX (CX-137), which causes depletion of FACT from sites of active transcription (Gasparian et al., 2011).

NGS of DNA fragments that coprecipitated with SSRP1 revealed a nonrandom genomic distribution of SSRP1 in HT1080 cells (Figures 3 and S5). Of SSRP1 peaks, 47% occurred near protein-coding genes, a distribution that is significant relative to a random target list ($p < 0.0001$). FACT distribution in relation to genome features is shown in Figure 3A and to TSS in Figure S5B. Gene-associated SSRP1 peaks were much more similar to broad RNA polymerase II peaks than to sharp peaks of sequence-specific TFs (Figure S5C). CX treatment substantially reduced association of FACT with genes (Figure 3A), confirming our previous findings that CX treatment depletes FACT from areas of gene transcription (Gasparian et al., 2011). As expected, SSRP1 bound NF-κB-dependent genes, and this binding was reduced after CX treatment (Gasparian et al., 2011; Figure S6). In total, we identified 2,085 genes in HT1080 cells with significant enrichment of SSRP1 over background (Table S1). For 93% of these genes, SSRP1 binding was reduced ($\geq$2-fold) after CX treatment. To strengthen our gene enrichment analysis, we selected 267 genes with SSRP1 binding >10-fold over background (200 kB around the TSS) that were significantly CX sensitive (Table S1).

Functional annotation of the list of SSRP1-enriched genes was accomplished by assessing overlap with the Molecular Signature Database (MSigDB, Broad Institute, Harvard University, MIT) curated gene lists. We obtained 52 lists with significant overlap ($p < 1.0 \times 10^{-5}$; FDR <0.05), which we divided into several functional categories (Tables 1 and S2): (1) MYC related; (2) stress induced (by UV, hypoxia, TNF, or genotoxic drugs); (3) cancer related (changed in cancer versus normal samples or in high-grade versus low-grade cancers); (4) meiosis and ribosome related, (5) growth factor induced; (6) associated with dedifferentiation; and (7) miscellaneous (including genes associated with system lupus erythematous [chronic inflammation], genes involved in the cell cycle, genes bound or upregulated by E2F TFs, and several other categories). This set of functional attributes suggests that FACT may be important for regulating expression of genes that stimulate proliferation, inhibit differentiation, and/or control stress responses.

As shown previously for NF-κB, FACT may control expression of the SSRP1-associated genes through interactions with particular TFs. To identify such TFs, we compared our list of SSRP1-enriched genes with (1) a list of genes with promoters containing

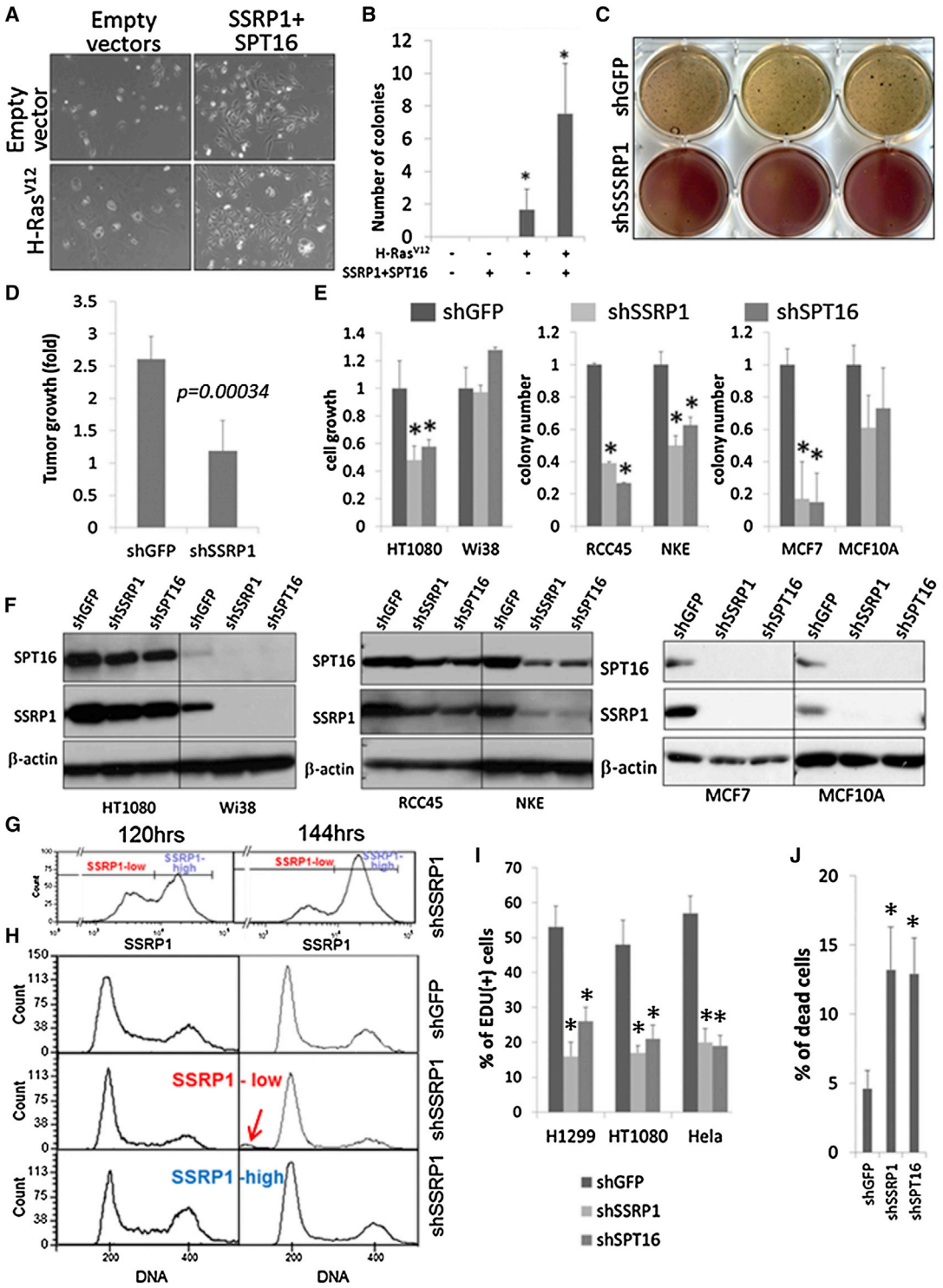

Figure 2. Transformation and Tumor, but Not Normal, Cell Growth Require FACT Expression

(A and B) Overexpression of FACT increases the efficiency of transformation of MCF10A cells by *H-Ras*^{V12}. (A) Microphotographs of 2D colonies 6 days after transduction of MCF10A cells with the indicated constructs. (B) Number of colonies in semisolid medium for MCF10A cells transduced with the indicated constructs or empty vectors (–), the mean of triplicates + SD; *$p < 0.05$ for comparison to cells transfected with both empty vectors.

(C and D) KD of SSRP1 suppresses *H-Ras*^{V12}-induced transformation of MCF10A cells. (C) MTT-stained colonies in semisolid medium in triplicate wells grown for 37 days after transduction of MCF10A cells with shRNAs. The darker color of shSSRP1 wells is due to unreduced MTT. (D) Growth of tumors (n = 10) in SCID mice

(legend continued on next page)

sequence elements known as TF binding sites using MSigDB (Table S3), and (2) lists of TF target sequences known from the literature using GenGo (Thomson Reuters) (Table S4). TFs identified by both methods are shown in Figure 3C. Most have well-established associations with cancer or embryonic development; importantly, all except one (TP53) promote tumor growth as oncogenes (MYC, JUN, Ets-family, YY1), inducers of cell proliferation (SP1, CREB, SRF), suppressors of apoptosis (NF-κB), or inhibitors of cell differentiation (OCT1, OCT4). Moreover, analysis of associations of SSRP1-enriched genes with disease states using GeneGo showed that most significant associations were with different types of neoplasms (Figure 3B).

In addition, we found that genes for several TFs including *MYC*, *JUN*, *JUNB*, *JUND*, *FOSL1*, and *FOSL2* (but not *TP53*) were themselves significantly "SSRP1 enriched" (Figure 3D). Thus, FACT may affect expression of some TFs themselves in addition to their targets.

FACT Subunits Are Overexpressed in Multiple Types of Tumors

To evaluate the clinical significance of our in vitro findings, we compared *SSRP1* and *SPT16* mRNA levels in human tumor and normal tissue using publicly available high-content microarray data and In Silico Transcriptomics Online-Integrated gene expression reference database (IST) Online software (MediSapiens) for transtechnology and transstudy normalization. This revealed that *SSRP1* mRNA, whereas showing significant variability among different samples, was elevated in the majority of tumors as compared to tissue from patients with no disease or noncancer-related diseases (Figure 4). Cultured cell lines included in the analysis had the highest average level of *SSRP1* of any category (Figure 4A), suggesting that in vitro conditions either induce *SSRP1* expression or select cells with elevated *SSRP1*.

SPT16 mRNA was also elevated in tumors, but to a lesser extent than *SSRP1* (Figure S7). This difference was consistent with our finding that *SSRP1* mRNA and protein both increased in the process of HMEC transformation, whereas for *SPT16*, only protein (not mRNA) levels increased (Figures 1B and 1C). This is most likely due to the demonstrated dependence of SPT16 protein levels on SSRP1 (Safina et al., 2013). Nevertheless, as for *SSRP1* mRNA, a significant number of tumors with very high levels of *SPT16* mRNA were observed among various types of cancer.

As a more direct evaluation of FACT expression in a clinical setting, we performed immunohistochemistry (IHC) staining of SSRP1 on tissue microarrays (TMAs) containing primary and metastatic tumors of different types as well as matching normal tissue from 793 patients (see Experimental Procedures). Tumors on the TMAs included invasive breast ductal and lobular carcinoma, non-small-cell lung cancer (NSCLC), renal cell carcinoma (RCC), and prostatic, pancreatic ductal (PDA), and colorectal adenocarcinomas. SSRP1 staining was used to assess FACT levels based on the previously established strong correlation between SSRP1 and SPT16 protein levels (Garcia et al., 2011). SSRP1 staining was scored using a semiquantitative system reflecting both the intensity of staining and the proportion of positive cells (see Experimental Procedures). On the TMAs, all cells in normal tissue samples were SSRP1 negative, with the exception of epithelial cells at the bottom of intestinal crypts (Figures 5A–5C; Garcia et al., 2011). Similarly, whereas tumor samples were frequently SSRP1 positive (see below), stromal cells present in the sample, constituting the tumor microenvironment, were invariably SSRP1 negative (Figures 5A–5C). The highest incidences of SSRP1-positive samples were observed in NSCLC (45%–63%), PDA (59%) and colon adenocarcinoma (50%) (Figure 5D). In contrast, very few cases of prostatic adenocarcinoma and RCC were SSRP1 positive (<10%) (Figure 5D). Therefore, we deemed the cohort of lung, pancreatic, and colon cancers to be "high SSRP1 expressors," whereas prostate and kidney cancers appear to be "low SSRP1 expressors." Notably, all cancers categorized as high SSRP1 expressors have a much lower overall survival rate as compared to low SSRP1 expressors. In line with this, invasive ductal carcinoma of the breast, which has an intermediate survival rate, was found to have an intermediate incidence of SSRP1-positive/-high samples (18%/13%). In contrast to the 100% incidence of SSRP1 expression in human tumor cell lines in vitro, but consistent with our mRNA expression data, a certain proportion of all tumor types were observed to have no SSRP1 staining (Figure 5D).

Correlation of FACT Levels with Clinicopathological Features of Tumors

Having established that some tumors are SSRP1 and SPT16 positive, whereas others are not, we evaluated whether FACT subunit expression correlated with any clinicopathological features of different types of tumors. Analysis of SSRP1 is described below; analysis of SPT16 shown in Extended Experimental

30 days after inoculation of mice with MCF10A cells transduced with the indicated shRNAs (bars indicate the mean fold tumor volume at day 30 to day 1 after inoculation; p value (t test) is shown.

(E) Growth of tumor (HT1080, RCC45, MCF7) and nontumor (WI38, NKE, MCF10A) cells after shRNA transduction/puromycin selection. Bars show the mean of triplicates of methylene blue staining (HT1080/Wi38) or colony number (RCC45/NKE, MCF7/MCF10A) ± SD, normalized to shGFP data in the same cell type. *$p < 0.05$.

(F) Western blot detection of FACT subunits in the cells described in (E) after puromycin selection.

(G) FACS analysis of SSRP1 staining in HT1080 cells 120 and 144 hr after transduction with shSSRP1.

(H) Cell-cycle distribution (FACS with DAPI staining) of HT1080 cells 120 hr (left column) and 144 hr (right) after transduction with shGFP or shSSRP1, with the latter population separated based on SSRP1 staining as shown in (G).

(I) EDU incorporation indicative of DNA replication 3 days after transduction of cells with the indicated shRNAs. *$p < 0.05$ for comparison to data with shGFP transduction in the same cells.

(J) Proportion of dead cells detected using Annexin V and propidium iodide staining (double positive) among HT1080 cells 5 days after transduction with the indicated shRNAs. *$p < 0.05$ for comparison to shGFP cells.

See also Figure S2.

A

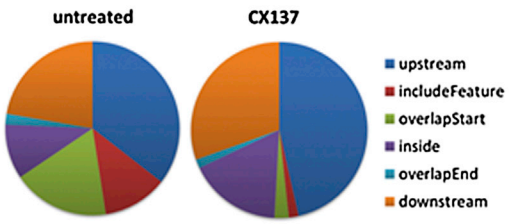

B

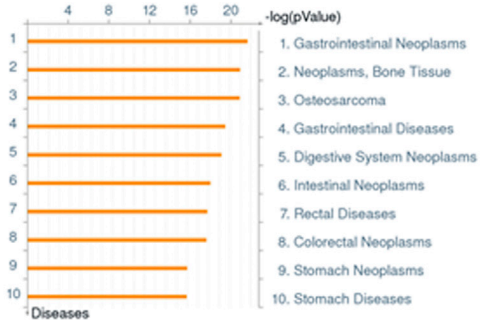

C

Transcription factors involved in the regulation of expression of SSRP1-enriched genes

TF family	TF	Major functional role	Defined role in cancer	References (reviews)
OCT	OCT1, OCT3/4	early embryonic development	OCT3/4 is overexpressed in poorly differentiated cancers	Chiou et al., 2008, Wen et al., 2013
AP1 binding	JUN, ATF1, ATF2, ATF3,	Proliferation	several members are oncogenes	Eychene et al., 2008, Gozdecka and Breitwieser, 2012
EGR	EGR1	Differentiation, mitogenesis	oncogenic or tumor suppressor	Pagel and Deindl, 2011
ets	ETS1, ELK1,	induction of proliferation	oncogenes	Shaikhibrahim et al., 2012
Myc and myc binding	Myc, Max, Maz, Myb	proliferation	oncogenes	Dang, 2012
NF-κB	Rel, RelA	inflammation, negative regulation of apoptosis	promotion of tumorigenesis	Gudkov et al., 2011
CREB	CREB1, CEBPA, CEBPB,	various	promotes proliferation of tumor cells	Xiao et al., 2010
TP53	TP53	control of genomic stability	tumor suppressor	Lane and Levine, 2010
Sp/KLF family	Sp1	early development	inductor of cell proliferation, positive regulation of tumor cell	Li and Davie, 2010
SRF	SRF	cell cycle regulation, apoptosis, cell growth, and	promotes proliferation and invasion of tumor cells	Kim et al., 2011
GLI-Kruppel	YY1	various	oncogene	Nicholson et al., 2011

D

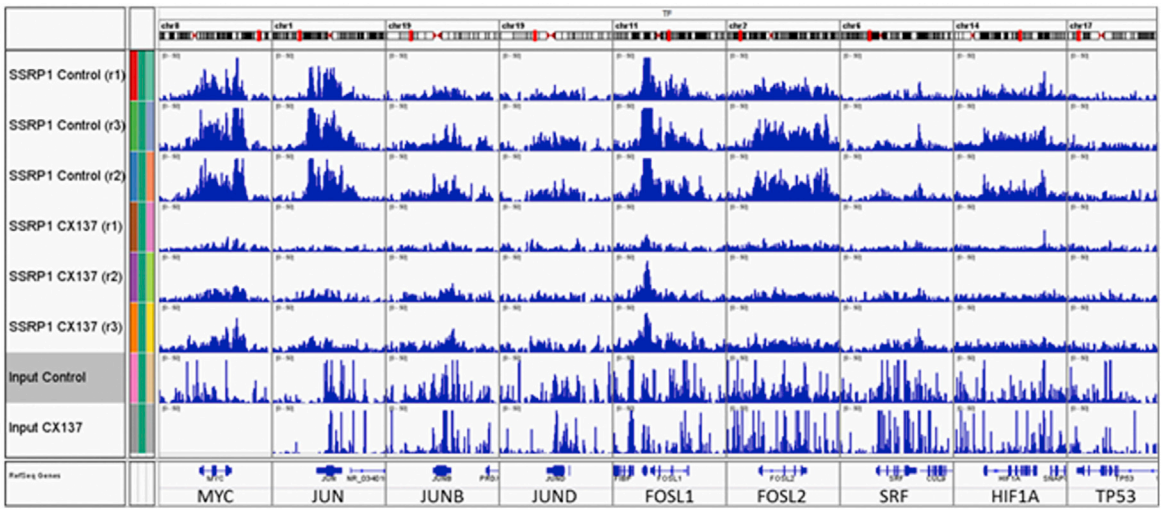

(legend on next page)

Procedures was generally concordant with SSRP1 (Figures S7, S8, S9, S10, S11, and S12). No correlation between tumor stage and *SSRP1* mRNA or protein level was found in any of the analyzed tumor types. This suggests that expression of FACT subunits is an early event in tumorigenesis and does not change with tumor growth (Table S5; Figures S8, S9, S10, S11, and S12). However, several cancers (breast, lung, and colon) showed a correlation between tumor grade and FACT expression, with significantly higher levels of *SSRP1* mRNA and protein in high-grade, poorly differentiated tumors (Table S5; Figures 6C, 6D, S8C, S9F, S11D, and S11E).

Among patients with breast cancer, *SSRP1* mRNA was higher in all tumor types versus normal breast tissue (Figure 6A) and in basal versus luminal carcinomas (Figure 6B). SSRP1 protein expression was more frequent in triple-negative versus hormone receptor-positive tumors and in ER-negative and Her2-positive versus ER-positive and Her2-negative tumors (Figure 6D; Table S5). Similarly, *SSRP1* mRNA was higher in NSCLC than in normal lung, and the highest level was observed in undifferentiated large-cell carcinomas (Figures S9A and S9C). The same tendency, although not statistically significant, was observed for SSRP1 protein (Figure S9E). Notably, among different histological subtypes of breast cancer and NSCLC, high SSRP1 expressors were generally tumor subtypes with worse prognoses than low SSRP1 expressors.

Because most cancer-related deaths are due to metastatic rather than primary disease, we evaluated whether SSRP1 expression is associated with metastatic disease. We found that patients with breast cancer and with RCC with SSRP1-positive primary tumors had a higher incidence of metastatic disease than patients with SSRP1-negative primary tumors (Figures 6D and S10D). In addition, *SSRP1* mRNA was higher among patients with metastases of lung and prostate cancers than among patients with no metastasis (Figures S9D and S12A). Overall, there was a strong correlation of SSRP1 status between primary and metastatic lesions in all cancers analyzed by IHC (97%). Therefore, the presence of SSRP1 in primary tumors of several types (e.g., breast) may be predictive of metastatic disease.

The data described above suggested that SSRP1 expression might be associated with tumor aggressiveness. To test this, we performed a correlation analysis between SSRP1 protein level and overall survival for all patients as a single cohort regardless of their tumor classification. To determine whether a particular degree of SSRP1 overexpression had prognostic value, we compared the following groups (defined by semiquantitative score cutoffs; see Experimental Procedures): (1) "high" SSRP1 versus "low" and negative samples, (2) positive SSRP1 versus weak/negative samples, and (3) SSRP1-negative versus all positive samples. For all tumor types, the strongest correlation between survival and SSRP1 level was obtained if SSRP1-positive and -negative samples were compared (Figures 5E and S13A). For all 793 patients, SSRP1 positivity was significantly associated with worse overall survival (Figure 5E). The same tendency, although not statistically significant, was observed in lung and colon cancers (Figure S13). In the tumors of patients with breast cancer, expression of SSRP1 was significant prognostic markers of poor survival based on univariate analysis (Figure S13D). The multivariate analysis of SSRP1 and hormone receptors status in breast cancer did not reveal SSRP1 as an independent marker with the number of patients we analyzed, but combination of SSRP1 with estrogen and progesterone receptors significantly improves the predictive value of both the established markers (Figures 6E and 6F). In summary, analysis of clinical samples indicated that SSRP1 is expressed more frequently and at a higher level in less-differentiated (higher grade) and more aggressive tumors, including (1) types of solid tumors with poor prognosis (lung, pancreatic, and colon); (2) histological subtypes of breast cancer and NSCLC with poor prognosis (triple negative, Her2 positive, large undifferentiated lung carcinoma); (3) metastatic tumors (breast, lung, renal, and prostate cancers); and (4) tumors from patients with low overall survival.

DISCUSSION

Although we and others previously noted elevated expression of FACT in tumor cell lines and in ovarian cancer patient samples (Gasparian et al., 2011; Hudson et al., 2007; Koman et al., 2012), this study provides a comprehensive analysis of FACT's value as a cancer marker and target. First, we found that both FACT subunits were elevated upon in vitro transformation of fibroblasts and epithelial cells induced by different agents (Figures 1 and S1). These data, together with the already-published observation that FACT is elevated upon *Her2/neu*-induced transformation of mammary epithelial cells (Koman et al., 2012), suggest that FACT upregulation may be a universal event during in vitro transformation. In epithelial cells, but not fibroblasts, the intermediate step of immortalization was accompanied by modest FACT elevation (Figure 1A); however, the most critical increase in both cell types coincided with transformation and acquisition of malignant properties, such as AIG and/or in vivo tumor growth (Figures 1A–1C, S1B, and S1C). Similarly, ectopic FACT expression induced growth in 2D cultures for epithelial cells, but not fibroblasts, while increasing the proportion of cells able to grow in semisolid medium for both cell types (Figures 2A–2C, S1D, and S1E). Because the same oncogene was used to transform both cell types, these data likely reflect cell-type-specific requirements for FACT during transformation.

Figure 3. Analysis of Genome-wide Distribution of SSRP1 in Tumor Cells

(A) MACS statistics of the distribution of SSRP1 tags in relation to genomic features in HT1080 cells untreated or treated with 3 μM CX-137 for 1 hr.

(B) GeneGo analysis of association of SSRP1-enriched genes with diseases; p values are shown, FDR <0.05.

(C) Families of TFs involved in regulating expression of SSRP1-enriched genes (see details in the text and full lists in Tables S1 and S2).

(D) Enrichment of SSRP1 binding to TF genes. Data are shown as alignments of SSRP1-bound DNA sequencings from three independent ChIP experiments with HT1080 cells left untreated (control, replicates r1–r3) or treated with CX (CX-137, replicates r1–r3) visualized using IGV.

See also Figures S3, S4, S5, and S6 and Tables S1, S2, S3, and S4.

Table 1. Curated Gene Lists from MSigDB Significantly Overlapping with the List of SSRP1-Enriched Genes Organized in Functional Categories

Functional Category	Gene Set Name	p Value
MYC related	Dang bound by MYC	0.00×10^{0}
	Dang MYC targets up	0.00×10^{0}
	Benporath MYC targets with E box	5.58×10^{-14}
	Benporath MYC max targets	1.96×10^{-12}
	GGGAGGRR V$MAZ Q6	8.47×10^{-9}
	LEI MYB targets	9.08×10^{-9}
Stress induced	ENK UV response keratinocyte up	0.00×10^{0}
	Dazard response to UV NHEK up	1.11×10^{-16}
	Krieg hypoxia not via knockdown M3A	1.75×10^{-10}
	HU genotoxic damage 24 hr	2.56×10^{-9}
	Winter hypoxia metagene	7.04×10^{-9}
	Harris hypoxia	1.41×10^{-8}
	Phong TNF targets up	2.05×10^{-8}
	Dazard UV response cluster G2	2.25×10^{-8}
Cancer related	Wang tumor invasiveness up	0.00×10^{0}
	Grade colon cancer up	1.11×10^{-16}
	Osman bladder cancer DN	3.89×10^{-15}
	CHNG multiple myeloma hyperploid up	6.55×10^{-15}
	LI amplified in lung cancer	7.78×10^{-11}
	Zucchi metastasis DN	7.31×10^{-10}
	Nutt GBM vs AO glioma DN	9.06×10^{-10}
	Sweet lung cancer kras UP	2.82×10^{-9}
	Acevedo liver cancer DN	3.51×10^{-9}
	Diaz chronic meylogenous leukemia DN	4.35×10^{-8}
Meiosis	Reactome meiosis	0.00×10^{0}
	Reactome meiotic recombination	0.00×10^{0}
	Reactome meiotic synapsis	3.15×10^{-14}
Ribosome	Kegg ribosome	0.00×10^{0}
	MIPS ribosome cytoplasmic	0.00×10^{0}
	MIPS 60S ribosomal subunit cytoplasmic	0.00×10^{0}
	MIPS 40S ribosomal subunit cytoplasmic	2.22×10^{-16}
Stimulated by growth factors	Nagashima EGF signaling up	8.58×10^{-13}
	Amit EGF response 40 hela	1.58×10^{-11}
	Nagashima NRG1 signaling up	6.56×10^{-11}
	Pedersen metastasis by ERBB2 isoform 1	1.12×10^{-9}
Chromatin organization	Reactome deposition of new cenpa-containing nucleosomes at the centromere	1.11×10^{-16}
	Reactome chromosome maintenance	3.33×10^{-12}
Differentiation	Benporath SOX2 targets	4.74×10^{-9}
	ESC V6.5 up early.V1 DN	7.69×10^{-7}
	ESC J1 up early.V1 DN	9.86×10^{-6}

Only lists with $p < 0.00 \times 10^{-6}$ are shown.
See also Tables S1, S2, S3, and S4.

Overexpression and shRNA-mediated KD experiments demonstrated that FACT was not simply correlated with transformation but functionally required. However, enforced expression of FACT was not able to substitute for H-Ras^{V12} in driving malignant transformation. This indicates that FACT-mediated chromatin changes are not sufficient to cause transformation but, rather, appear to create conditions that promote or accelerate the oncogenic activity of other factors. Therefore, FACT cannot be categorized as an oncogene or "driver" of malignant transformation, but at the same time, it is not a "passenger." We suggest the term "accelerator" or factor that makes the function of a driver more efficient.

FACT remains important even in established tumors, as illustrated by our finding that all tested tumor cell lines were sensitive to FACT KD (Gasparian et al., 2011; Figures 2 and S2). Unlike normal and immortalized nontransformed cells, tumor cell lines with reduced levels of FACT could not be expanded (Figures 2F and S2). Selective FACT dependence of tumor, but not normal, cells indicates that targeting of FACT could be a safe and effective anticancer strategy.

However, many patient tumor samples are FACT negative, indicating that FACT is not universally important for tumor transformation in vivo. Most normal tissues in vivo, as well as normal primary cells in culture, are FACT negative. Passaging of these cells in vitro results in elevation of FACT levels (unpublished data), suggesting that for normal cells, either in vitro stress induces FACT expression, or only cells with elevated FACT (stem or undifferentiated progenitor cells as shown in Garcia et al., 2011) can grow in culture. Both of these possibilities are consistent with our observation that many FACT-controlled genes are either involved in the maintenance of pluripotent cell state or induced by different types of cellular stress (Table 1), and there may be a feedback mechanism between stress and FACT expression. In line with this hypothesis, all tested cultured tumor cell lines were FACT positive (Garcia et al., 2011; Gasparian et al., 2011), whereas many patient tumor samples were FACT negative. Furthermore, *SSRP1* and *SPT16* mRNA levels were consistently higher in cultured cell lines as compared to practically all tissues in vivo (Figures 4 and S7).

Thus, our data show that normal and tumor cells can be either FACT positive or negative in vivo, whereas both categories are FACT positive in vitro (although to different extents). The key

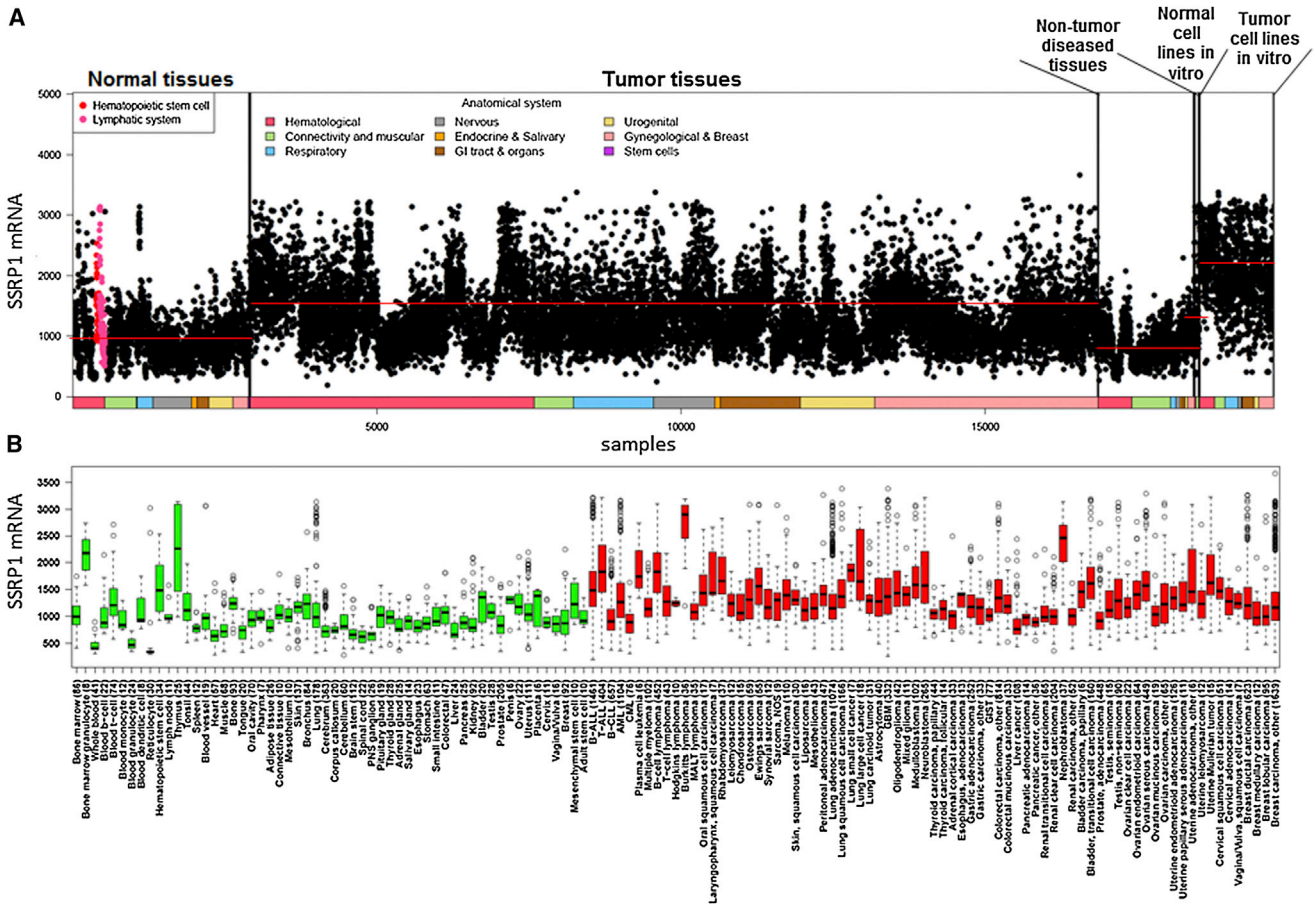

Figure 4. *SSRP1* mRNA Expression in Patient Samples and Cultured Cell Lines

(A) Dot plot of normalized *SSRP1* mRNA levels (y axis; see details in Experimental Procedures) in all analyzed samples (x axis, n = 20,000) shown in an anatomically and pathologically ordered fashion (x axis colors correspond to the legend at top of panel). Colored dots are those with an expression level 1 SD higher than the average expression in all samples of the same type (normal, tumor, nontumor diseased, etc., as shown above panel) or those in which the 90th percentile of expression was more than two times the interquartile range plus the 75th percentile of the same type. However, no anatomy or cancer type is colored if there were fewer than ten data points per tissue type. Red lines indicate median for each sample category.

(B) Tissue box-whisker plot of *SSRP1* expression in samples of nondiseased (healthy) and cancer tissues. All results with at least five samples are shown. Green boxes indicate nondiseased samples, whereas red boxes indicate cancer(s). Boxes span the 25th–75th percentile of the data with the horizontal line at the median. The whiskers extend to 1.5 times the interquartile range from the edges of the box, and any data points beyond this were considered outliers (hollow circles). See also Figure S7.

difference between these cell types is that tumor cells are sensitive to FACT inhibition, whereas normal cells are not (Figures 2 and S2). This was also true in vivo because inhibition of FACT activity by CXs had antitumor effects in multiple mouse models at nontoxic concentrations (Gasparian et al., 2011).

To extend the relevance of our findings in cultured cells (see above) and in CX-treated mice toward patients with cancer, we investigated FACT expression in a large number of human normal and tumor tissue samples via (1) analysis of publicly available microarray-based gene expression data sets, and (2) IHC staining of TMAs containing an independent set of samples. The bioinformatics approach first suggested that FACT may not be a universal cancer marker because not all tumor samples displayed elevated FACT levels (Figures 4 and S7). Trying to clarify the difference between tumors with low and high levels of FACT, we noticed that the most significant association with clinical features was between FACT-positive and -negative tumors. Thus, whether tumor cells express FACT or not appears to be more important than the level of expression. Notably, multiple specific subtypes of tumors had a high incidence of FACT positivity, and almost universally, these subtypes behaved more aggressively (overall survival of patients with FACT-positive tumors was significantly worse than that of patients with FACT-negative tumors; Figure 5E).

In line with FACT expression in normal mouse and human tissues being limited to stem and undifferentiated progenitor cells, FACT expression was positively correlated with grade for several cancer types (Table S5). This suggests that FACT is mostly expressed in poorly differentiated tumors. We did not observe this correlation in PDA; however, our PDA sample set did not include any well-differentiated tumors, only moderately and poorly differentiated ones (which are aggressive, have poor

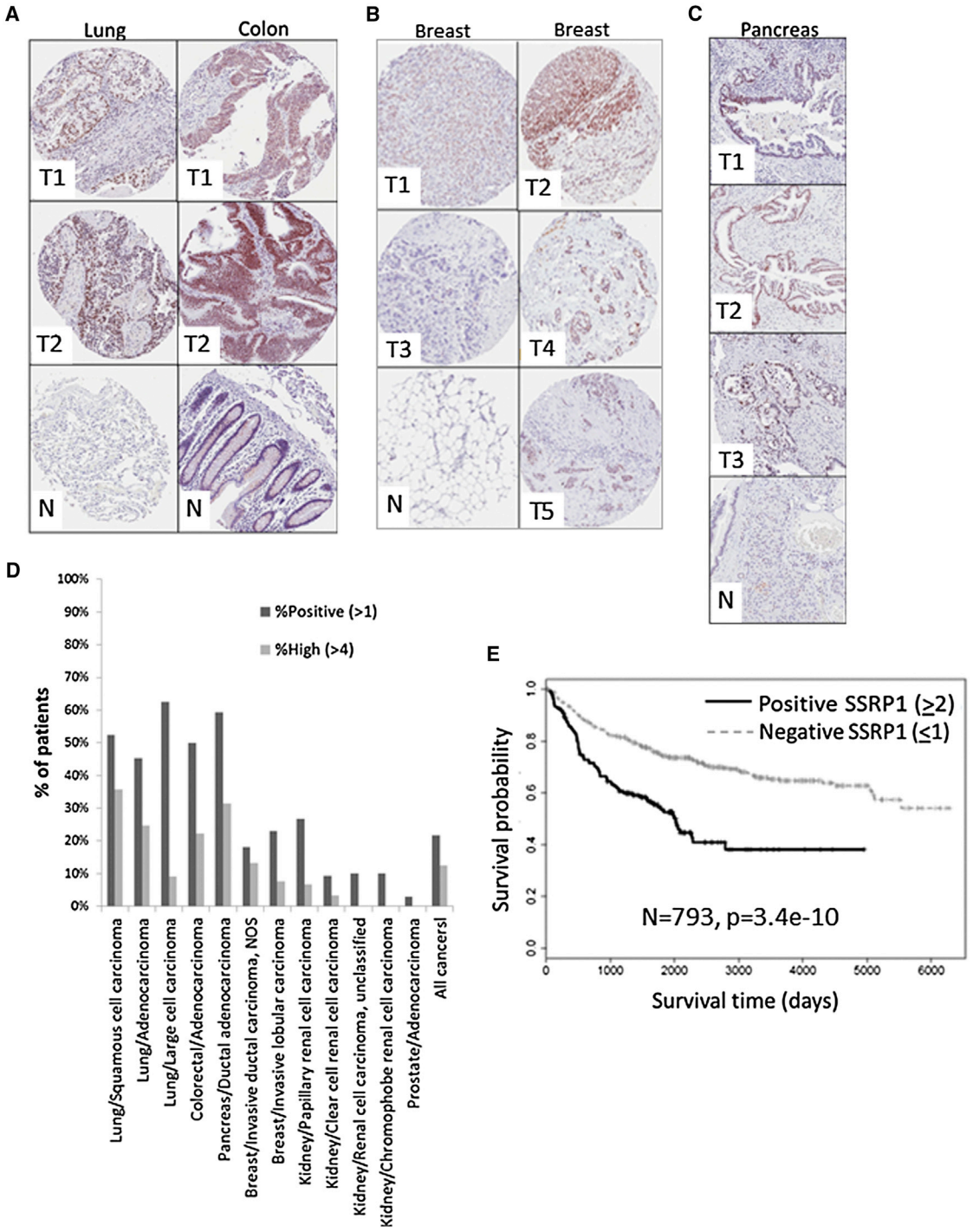

Figure 5. SSRP1 Protein Expression in Human Tumors Is Associated with Poor Overall Patient Survival

(A–D) Examples of IHC staining with antibodies to SSRP1 containing normal (N) and tumor (T) tissues of lung and colon (A), breast (B), and pancreatic (C) tissues. (D) Proportion of patients with SSRP1 expression in their tumors ("Positive" indices are more than one, and "High" indices are more than four; te scoring system is described in Experimental Procedures) out of all analyzed patients with the same type of cancer.

(E) Patients with SSRP1-negative tumors have better overall survival. Kaplan-Meier survival curves were built using data for all analyzed patients (n = 793). The p value was calculated using the log rank test.

See also Figure S13 and Table S5.

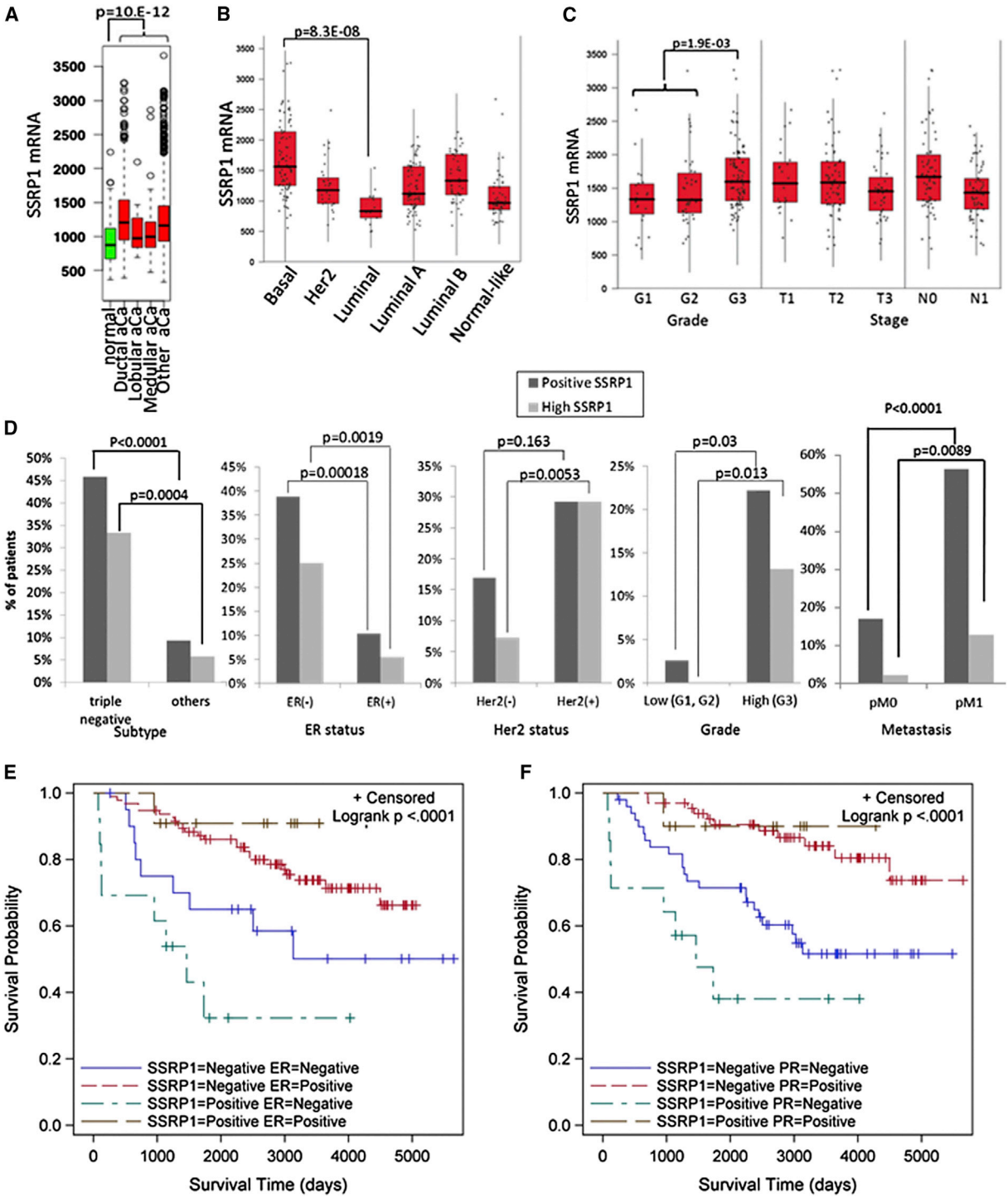

Figure 6. SSRP1 mRNA and Protein Expression in Breast Cancer

(A–C) Box-whisker plots of *SSRP1* mRNA levels in (A) samples of breast tissue (aCa, adenocarcinoma); (B) breast cancer samples categorized by gene expression signature; and (C) breast cancer samples of different grades and stages. p Values from Mann-Whitney-Wilcoxon tests between indicated samples are shown. p Values >0.05 are not shown.

(D) Comparison of the proportion of SSRP1-positive samples (based on IHC staining) among patients within different categories of breast cancer. The p values from exact Fisher chi-square tests between different categories are shown.

(E and F) Combination of SSRP1 expression with negative ER (E) and PR (F) status is a significant predictor of poor survival in patients with breast cancer. Kaplan-Meier survival curves for each combination of markers.

See also Figures S8, S9, S10, S11, and S12.

prognosis, and consistent with our hypothesis, were frequently FACT positive).

Further supporting the association of FACT with tumor aggressiveness, FACT expression was found to be significantly correlated with metastasis of breast, renal, and prostate cancer. Importantly, the FACT status (SSRP1 staining on TMA) of the primary tumor was associated with the development of metastatic disease. This, together with the lack of correlation between FACT expression and tumor stage or timing, increases the potential value of FACT as a prognostic marker because FACT positivity of a primary tumor could be used at a very early stage to determine the risk for future metastatic disease.

Although all of our data indicate that the SSRP1 and SPT16 subunits of FACT are coordinately expressed in cancer, SSRP1 is the most promising candidate for a diagnostic/prognostic marker because its upregulation is more obvious on both the mRNA and protein levels. This likely derives from the unusual mechanism of SSRP1 and SPT16 coregulation that we recently described in which the stability of both proteins depends upon formation of the FACT complex, and stability of the complex is determined by the presence of *SSRP1* mRNA (Safina et al., 2013). In this way, an increase of SSRP1 mRNA is sufficient to drive elevation of both SSRP1 and SPT16 proteins. This was confirmed in the in vitro transformation experiments reported here: whereas only *SSRP1* (not *SPT16*) mRNA was elevated in all transformed cells, protein levels of both SSRP1 and SPT16 were increased (Figures 1A–1C). This same trend was noted in many types of tumors: *SSRP1* mRNA was increased much more universally than *SPT16* mRNA (Figures 4, 6, S7, S8, S9, S10, S11, and S12). At the same time, we did observe tumors with significantly increased *SPT16* mRNA (Figure S7). In the future, it will be interesting to analyze whether these tumors have any selective advantages over those in which only *SSRP1* mRNA is elevated.

The mechanism(s) underlying FACT's role as an accelerator of transformation remains to be fully elucidated. However, our previous demonstration that FACT-assisted NF-κB-dependent transcription is involved suggested that modulation of transcriptional programs driven by other TFs might also contribute to FACT's procancerous effects. Support for this hypothesis was gained through our ChIP-based exploration of the distribution of chromatin-bound SSRP1. This confirmed significant and selective association of FACT with protein-expressing genes (Figures 3A, 3D, and S5). SSRP1 peak distribution over the whole body of genes, with additional enrichments at the start and end of the gene territory, indicated involvement of FACT in transcription initiation, elongation, and possibly termination. The selectivity of FACT in assisting the transcription of some, but not other, genes was previously demonstrated through comparison of gene expression profiles in yeast (reviewed in Formosa, 2012), plant, and mammalian cells following inactivation of FACT (Duroux et al., 2004; Li et al., 2005; Lolas et al., 2010).

The list of SSRP1-enriched genes obtained in our study contains many "procancer" genes, including numerous TF targets involved in induction of proliferation, inhibition of cell death and differentiation, maintenance of cell pluripotency, and stress responses (Tables 1, S2, S3, and S4; Figures 3C and 3D). The mechanism by which FACT selects these genes is currently under study, although FACT has been found among the direct interactors of several TFs that, based upon SSRP1 binding to their genes, may require FACT for expression (i.e., MYC, SRF, and OCT4) (Bunker and Kingston, 1995; Kihara et al., 2008; Spencer et al., 1999; Pardo et al., 2010; van den Berg et al., 2010).

We also cannot exclude a nontranscription-related role for FACT in cancer. FACT is known to be involved in replication, and replication is clearly reduced upon FACT KD. However, the availability of cells in vivo and in vitro that can replicate without FACT suggests that this may not be the only FACT-dependent process that is vital for tumor cells. Additional reported functions of FACT that might contribute to its role in cancer are regulation of DNA damage responses and DNA repair. However, genes involved in these processes are usually lost or mutated in cancer (e.g., *BRCA*, *MHS*), whereas neither *SPT16* nor *SSRP1* displays higher-than-background incidences of mutations or deletions in any type of cancer (TCGA, cBio portal). SSRP1, but not SPT16, was reported to be required (in cooperation with many other factors) for proper spindle formation during mitosis (Zeng et al., 2010). We cannot exclude that elevation of SSRP1, and concomitantly SPT16, levels may be due to the increased rate of mitosis in cancer cells; however, it seems unlikely that an artificial increase in FACT expression would induce transformation by assisting with spindle formation. Understanding the mechanism(s) by which FACT promotes cancer is a major goal of our current work.

In conclusion, the results of this study indicate that FACT is a promising marker and target for subtypes of cancer characterized by high grade and aggressiveness and poor prognosis. This, together with the absence of FACT expression in most normal cells/tissues, suggests that pharmacological inhibition of FACT could be a safe and effective strategy to treat types of cancer for which there are currently few treatment options.

EXPERIMENTAL PROCEDURES

Reagents

CX-137 (CBLC137) was provided by Cleveland BioLabs.

Cells

HT1080, WI-38, MCF7, and MCF10A cells were obtained from ATCC and maintained as suggested. RCC45 and NKE-hTERT cells have been described (Gurova et al., 2004).

HMECs were obtained from Martha Stampfer (Lawrence Berkeley National Laboratory) and modified and maintained as described by Garbe et al. (2009). 184B5 and 184AA3 were immortalized following exposure to benzo(a)pyrene (Stampfer and Bartley, 1985; Stampfer et al., 2003); 184Dp16sMY and 240Lp16sMy were immortalized following transduction of *c-Myc* and shRNAs against p16; 184FMY2 immortalized via expression of *c-Myc*. The immortalized BJ fibroblast cell line with tamoxifen-regulated *H-Ras* ^{V12} was obtained from Reuven Agami (The Netherlands Cancer Institute). Wild-type and p53-knockout MEF cells were obtained from 13.5-day pregnant C57/B6 wild-type or p53$^{-/-}$ mice and maintained in DMEM with 10% FBS and antibiotics.

Growth of cells in semisolid media was assessed as described by Yang et al. (2012). Colonies were counted unstained in ten blindly selected fields of view in each of three replicate wells using 10× phase-contrast microscopy or stained with 5 μg/ml MTT (Sigma-Aldrich) and photographed.

Growth of cells in SCID mice was done according to institution ethical committee-approved animal protocol. Five million shRNA-transduced MCF10A cells were subcutaneously inoculated into two sites of female 8-week-old

SCID mice (n = 5) in 50% Matrigel/PBS solution. Tumors were measured once a week using digital caliper, and volume was calculated using the formula V = length × width^2/2. Tumor growth was calculated as fold increase of tumor volume between days 1 and 30 after inoculation.

Plasmids, Transfection, and Lentiviral Transduction

pLV-H-Ras^{V12}-Bleo or pLV-Bleo lentiviral vectors were kindly provided by Dr. Andrei Gudkov (Roswell Park Cancer Institute [RPCI]). Human SSRP1 cDNA was cloned into the pLV-CMV-Neo lentiviral vector and verified by sequencing. *SPT16* cDNA was synthesized (Invitrogen; GeneArt AG) using a sequence optimized for protein expression by DAPCEL and cloned into the pMLV HygroR lentiviral vector. Mission shRNAs targeting *SSRP1* (TRCN0000019270), *SPT16* (TRCN0000001260), and *GFP* (SHC004) were obtained from Sigma-Aldrich.

siRNAs targeting *SSRP1*(On-Target plus SMART pool, catalog #L-011783-00) or *SPT16* (On-Target plus SMART pool, catalog #L-009517-00) and siCONTROL nontargeting siRNA (catalog #D-001210-01) were from Thermo Scientific Dharmacon. Transfection was performed using Lipofectamine 2000 reagent (Life Technologies). Lentivirus packaging and infection were conducted as described (Gurova et al., 2004, 2005).

Western blotting, fluorescent-activated cell sorting, and immunofluorescent staining were done as described (Gasparian et al., 2011; Gurova et al., 2004, 2005). The list of antibodies used can be found in Extended Experimental Procedures.

Replication and transcription rates in cells were measured using Click-iT EDU Alexa Fluor 594 HCS Assay and Click-iT RNA Alexa Fluor 488 HCS Assay kits (Invitrogen). Quantitative RT-PCR was done as described (Safina et al., 2013).

Patient Samples

Patients included in this study (n = 793) were diagnosed with cancer between March 1992 and January 2010 at RPCI. The RPCI institutional review board gave approval for this study. We selected all patients from this time period with adequate material in the RPCI archive for IHC and with follow-up information in the RPCI tumor registry or various RPCI research program databases. The 793 patients included 143 with invasive ductal carcinoma of the breast, 13 with invasive lobular carcinoma of the breast, 54 with colorectal adenocarcinoma, 10 with chromophobe RCC, 235 with clear-cell RCC, 15 with papillary RCC, 10 with RCC unclassified, 73 with lung adenocarcinoma, 11 with lung large-cell carcinoma, 42 with lung squamous cell carcinoma, 54 with ductal adenocarcinoma of the pancreas, and 133 with prostatic adenocarcinoma. Demographic details and number of patients with representative tumors are provided in Extended Experimental Procedures and Table S6.

TMAs

SSRP1 protein expression in the clinical cohort was assessed using 16 TMAs comprising six cancer types collected from patients described above. All RPCI TMAs are built in a standardized fashion with three 1 mm tissue cores from formalin-fixed paraffin-embedded donor blocks precisely arrayed into a new recipient paraffin block, including tumor specimens as well as controls. For most TMAs, three cores of matching normal tissue were also evaluated. Additional controls within each TMA consisted of multiple cores of normal tissue from ten different organs including heart, colon, kidney, adrenal, ovary, myometrium, brain, thyroid, lung, and prostate representing slightly more than 20% of all cores per TMA.

TMA Scoring

TMAs were stained as described (Garcia et al., 2011). Results were recorded according to the American Society of Clinical Oncology Guideline Recommendations. The neoplastic cells for any given core were scored in a semiquantitative/ordered categorical manner for intensity (range of scores 0–3) and percentage of cells: 0 (0%), 1 (1%–9%), 2 (10%–49%), 3 (50%–100%) staining. The results for all cores for one patient in a TMA format were averaged for a final score. An IHC index (range of scores 0–9) was defined as the product of the intensity and percentage of cells staining. Cores were excluded from evaluation due to an absence of tumor cells, or core drop-off. Cases were also excluded if there was insufficient clinical or outcome data.

Statistical Analysis of TMA Staining

The SSRP1 IHC data were dichotomized as described in the TMA Scoring section. Fisher's exact tests were performed to test the association between the dichotomized SSRP1 expression indices (0 versus all others; <2 versus ≥2; ≤4 versus >4) and other dichotomized categorical variables, such as age (≥60/<60), tumor grade (high/low), stage (early/late), and expression of disease-specific markers, where available. Chi-square tests were performed to test for association with categorical variables of more than two levels. Kaplan-Meier survival analyses with log rank tests (Peto and Peto, 1972) were employed to assess the correlation between patient survival and SSRP1 expression index. The p values <0.05 were considered significant. Multivariate survival analysis was conducted using Cox regression. All statistical analyses were performed using the R statistical programming language (R Team, 2012).

In Silico Analysis of SSRP1 and SPT16 Expression

Analysis of gene expression data from 251 different studies was performed using the IST Online. Details of this analysis are provided in Extended Experimental Procedures.

Immunoprecipitation of SSRP1/SPT16 Complex

HT1080 cells were lysed in NP40 buffer and rotated at 4°C for 15 min. Then, lysates were centrifuged at 14,000 × *g* for 15 min, and supernatants were precleared by rotating them with protein A/G agarose beads at 4°C for 1 hr. Cell lysates at 1 mg/ml concentrations were rotated overnight with anti-SSRP1 (catalog #609702; BioLegend) or control mouse IgG2b (catalog #400302; BioLegend) at 5 μg/500 μl lysate at 4°C. To capture immunocomplexes, Dynabeads Protein A (Life Technologies) were added to the lysates according to the manufacturer's instructions and then rotated for 1 hr at 4°C. Beads were collected, washed three times with cold PBS, and either used for LC/MS sample preparation or boiled in 60 μl of 2× loading buffer for 5 min, after being centrifuged briefly to separate the supernatants for SDS-PAGE and western blotting. Sample preparation for LC-MS/MS analysis, database search, and peptide and protein identification are described in Extended Experimental Procedures.

ChIP Sequencing and Analysis

ChIP was performed (three independent experiments) using HT1080 cells left untreated or treated with 3 μM CX-137 for 1 hr with the mouse monoclonal anti-SSRP1 (catalog #609702; BioLegend) and mouse IgG2b antibody (catalog #400302; BioLegend). ChIP was performed with a kit from Upstate (EMD Millipore) as outlined by the manufacturer except that Dynabeads Protein A (Invitrogen) were used instead of Protein A agarose beads. ChIP-isolated DNA was treated using the standard ChIP-sequencing protocol from Illumina except that after adaptor ligation, the library was separated on a 2% agarose gel, and the 150–500 bp region was excised and purified. The resulting ChIP libraries were single-end sequenced on an Illumina HiSeq 2000 with 50 bp reads. Each sample was sequenced in a single-flow cell lane and generated 89–190 million reads. The resulting raw sequencing reads were filtered for quality and aligned to the most recent build of the human genome (hg19) with BowTie. Peaks were identified, averaged, and normalized against the background, and input using PeakRanger (Feng et al., 2011). The peak positions in relation to genome features were calculated using MACS (Zhang et al., 2008). For this, the data from replicated samples were concatenated together. The comparison of peaks in untreated and CX-137-treated samples and peak annotation was performed using an Integrated Genomic Viewer (Broad Institute, MIH, Harvard University).

ACCESSION NUMBERS

Sequencing data in the form of bed files were deposited in the NCBI database under accession number GSE45393.

SUPPLEMENTAL INFORMATION

Supplemental Information includes Extended Experimental Procedures, 13 figures, and 6 tables and can be found with this article online at http://dx.doi.org/10.1016/j.celrep.2013.06.013.

ACKNOWLEDGMENTS

We would like to thank Dr. Bruce Specht for his constant and enormous support of our research, Dr. Andrei Gudkov for critical discussion of the work and manuscript, Dr. Patricia Stanhope Baker for editing of the manuscript, Daria Fleyshman for help with graphical work, Monica Murphy for help with organization of the clinical data, Jonathan Bard for help with processing of sequencing files, and Yekaterina Leonova for help with mouse embryonic fibroblasts. We also thank Natalia Tararova and Anton Komar from Dapcel for help with generation of SPT16 mammalian expression construct. Biospecimens and research pathology services for this study were provided by the Pathology Resource Network, which is funded by the National Cancer Institute (NCI) and is a RPCI Cancer Center Support Grant (CCSG) shared resource. Clinical Data Delivery and Honest Broker services for this study were provided by the Clinical Data Network, which is funded by the NCI and is a RPCI CCSG shared resource. This study was funded by grants from Incuron and The Komen Foundation (CCR13264604) to K.V.G.

Received: March 25, 2013
Revised: May 31, 2013
Accepted: June 7, 2013
Published: July 3, 2013

REFERENCES

Belotserkovskaya, R., Oh, S., Bondarenko, V.A., Orphanides, G., Studitsky, V.M., and Reinberg, D. (2003). FACT facilitates transcription-dependent nucleosome alteration. Science *301*, 1090–1093.

Birch, J.L., Tan, B.C., Panov, K.I., Panova, T.B., Andersen, J.S., Owen-Hughes, T.A., Russell, J., Lee, S.C., and Zomerdijk, J.C. (2009). FACT facilitates chromatin transcription by RNA polymerases I and III. EMBO J. *28*, 854–865.

Brenner, A.J., Stampfer, M.R., and Aldaz, C.M. (1998). Increased p16 expression with first senescence arrest in human mammary epithelial cells and extended growth capacity with p16 inactivation. Oncogene *17*, 199–205.

Bunker, C.A., and Kingston, R.E. (1995). Identification of a cDNA for SSRP1, an HMG-box protein, by interaction with the c-Myc oncoprotein in a novel bacterial expression screen. Nucleic Acids Res. *23*, 269–276.

Duroux, M., Houben, A., Růzicka, K., Friml, J., and Grasser, K.D. (2004). The chromatin remodelling complex FACT associates with actively transcribed regions of the *Arabidopsis* genome. Plant J. *40*, 660–671.

Feng, X., Grossman, R., and Stein, L. (2011). PeakRanger: a cloud-enabled peak caller for ChIP-seq data. BMC Bioinformatics *12*, 139.

Formosa, T. (2012). The role of FACT in making and breaking nucleosomes. Biochim. Biophys. Acta *1819*, 247–255.

Garbe, J.C., Bhattacharya, S., Merchant, B., Bassett, E., Swisshelm, K., Feiler, H.S., Wyrobek, A.J., and Stampfer, M.R. (2009). Molecular distinctions between stasis and telomere attrition senescence barriers shown by long-term culture of normal human mammary epithelial cells. Cancer Res. *69*, 7557–7568.

Garcia, H., Fleyshman, D., Kolesnikova, K., Safina, A., Commane, M., Paszkiewicz, G., Omelian, A., Morrison, C., and Gurova, K. (2011). Expression of FACT in mammalian tissues suggests its role in maintaining of undifferentiated state of cells. Oncotarget *2*, 783–796.

Gasparian, A.V., Burkhart, C.A., Purmal, A.A., Brodsky, L., Pal, M., Saranadasa, M., Bosykh, D.A., Commane, M., Guryanova, O.A., Pal, S., et al. (2011). Curaxins: anticancer compounds that simultaneously suppress NF-κB and activate p53 by targeting FACT. Sci. Transl. Med. *3*, 95ra74.

Gudkov, A.V., Gurova, K.V., and Komarova, E.A. (2011). Inflammation and p53: a tale of two stresses. Genes Cancer *2*, 503–516.

Gurova, K.V., Hill, J.E., Razorenova, O.V., Chumakov, P.M., and Gudkov, A.V. (2004). p53 pathway in renal cell carcinoma is repressed by a dominant mechanism. Cancer Res. *64*, 1951–1958.

Gurova, K.V., Hill, J.E., Guo, C., Prokvolit, A., Burdelya, L.G., Samoylova, E., Khodyakova, A.V., Ganapathi, R., Ganapathi, M., Tararova, N.D., et al. (2005). Small molecules that reactivate p53 in renal cell carcinoma reveal a NF-kappaB-dependent mechanism of p53 suppression in tumors. Proc. Natl. Acad. Sci. USA *102*, 17448–17453.

Heo, K., Kim, H., Choi, S.H., Choi, J., Kim, K., Gu, J., Lieber, M.R., Yang, A.S., and An, W. (2008). FACT-mediated exchange of histone variant H2AX regulated by phosphorylation of H2AX and ADP-ribosylation of Spt16. Mol. Cell *30*, 86–97.

Hudson, M.E., Pozdnyakova, I., Haines, K., Mor, G., and Snyder, M. (2007). Identification of differentially expressed proteins in ovarian cancer using high-density protein microarrays. Proc. Natl. Acad. Sci. USA *104*, 17494–17499.

Ikeda, Y., Kinoshita, Y., Susaki, D., Ikeda, Y., Iwano, M., Takayama, S., Higashiyama, T., Kakutani, T., and Kinoshita, T. (2011). HMG domain containing SSRP1 is required for DNA demethylation and genomic imprinting in *Arabidopsis*. Dev. Cell *21*, 589–596.

Keller, D.M., Zeng, X., Wang, Y., Zhang, Q.H., Kapoor, M., Shu, H., Goodman, R., Lozano, G., Zhao, Y., and Lu, H. (2001). A DNA damage-induced p53 serine 392 kinase complex contains CK2, hSpt16, and SSRP1. Mol. Cell *7*, 283–292.

Kihara, T., Kano, F., and Murata, M. (2008). Modulation of SRF-dependent gene expression by association of SPT16 with MKL1. Exp. Cell Res. *314*, 629–637.

Koman, I.E., Commane, M., Paszkiewicz, G., Hoonjan, B., Pal, S., Safina, A., Toshkov, I., Purmal, A.A., Wang, D., Liu, S., et al. (2012). Targeting FACT complex suppresses mammary tumorigenesis in Her2/neu transgenic mice. Cancer Prev. Res. (Phila.) *5*, 1025–1035.

Kumari, A., Mazina, O.M., Shinde, U., Mazin, A.V., and Lu, H. (2009). A role for SSRP1 in recombination-mediated DNA damage response. J. Cell. Biochem. *108*, 508–518.

Li, Y., Keller, D.M., Scott, J.D., and Lu, H. (2005). CK2 phosphorylates SSRP1 and inhibits its DNA-binding activity. J. Biol. Chem. *280*, 11869–11875.

Lolas, I.B., Himanen, K., Grønlund, J.T., Lynggaard, C., Houben, A., Melzer, M., Van Lijsebettens, M., and Grasser, K.D. (2010). The transcript elongation factor FACT affects *Arabidopsis* vegetative and reproductive development and genetically interacts with HUB1/2. Plant J. *61*, 686–697.

Pardo, M., Lang, B., Yu, L., Prosser, H., Bradley, A., Babu, M.M., and Choudhary, J. (2010). An expanded Oct4 interaction network: implications for stem cell biology, development, and disease. Cell Stem Cell *6*, 382–395.

Peto, R., and Peto, J. (1972). Asymptotically efficient rank invariant test procedures. J. R. Stat. Soc. Ser. A *135*, 185–207.

Reinberg, D., and Sims, R.J., 3rd. (2006). de FACTo nucleosome dynamics. J. Biol. Chem. *281*, 23297–23301.

R Team (2012). The R Project for Statistical Computing. http://www.r-project.org/.

Safina, A., Garcia, H., Commane, M., Guryanova, O., Degan, S., Kolesnikova, K., and Gurova, K.V. (2013). Complex mutual regulation of facilitates chromatin transcription (FACT) subunits on mRNA and protein levels in human cells. Cell Cycle. Published online June 28, 2013.

Saunders, A., Werner, J., Andrulis, E.D., Nakayama, T., Hirose, S., Reinberg, D., and Lis, J.T. (2003). Tracking FACT and the RNA polymerase II elongation complex through chromatin in vivo. Science *301*, 1094–1096.

Singer, R.A., and Johnston, G.C. (2004). The FACT chromatin modulator: genetic and structure/function relationships. Biochem. Cell Biol. *82*, 419–427.

Spencer, J.A., Baron, M.H., and Olson, E.N. (1999). Cooperative transcriptional activation by serum response factor and the high mobility group protein SSRP1. J. Biol. Chem. *274*, 15686–15693.

Stampfer, M.R., and Bartley, J.C. (1985). Induction of transformation and continuous cell lines from normal human mammary epithelial cells after exposure to benzo[a]pyrene. Proc. Natl. Acad. Sci. USA *82*, 2394–2398.

Stampfer, M.R., Garbe, J., Nijjar, T., Wigington, D., Swisshelm, K., and Yaswen, P. (2003). Loss of p53 function accelerates acquisition of telomerase activity in indefinite lifespan human mammary epithelial cell lines. Oncogene *22*, 5238–5251.

Tan, B.C., Chien, C.T., Hirose, S., and Lee, S.C. (2006). Functional cooperation between FACT and MCM helicase facilitates initiation of chromatin DNA replication. EMBO J. *25*, 3975–3985.

Tan, B.C., Liu, H., Lin, C.L., and Lee, S.C. (2010). Functional cooperation between FACT and MCM is coordinated with cell cycle and differential complex formation. J. Biomed. Sci. *17*, 11.

van den Berg, D.L., Snoek, T., Mullin, N.P., Yates, A., Bezstarosti, K., Demmers, J., Chambers, I., and Poot, R.A. (2010). An Oct4-centered protein interaction network in embryonic stem cells. Cell Stem Cell *6*, 369–381.

Yang, N., Morrison, C.D., Liu, P., Miecznikowski, J., Bshara, W., Han, S., Zhu, Q., Omilian, A.R., Li, X., and Zhang, J. (2012). TAZ induces growth factor-independent proliferation through activation of EGFR ligand amphiregulin. Cell Cycle *11*, 2922–2930.

Zeng, S.X., Li, Y., Jin, Y., Zhang, Q., Keller, D.M., McQuaw, C.M., Barklis, E., Stone, S., Hoatlin, M., Zhao, Y., and Lu, H. (2010). Structure-specific recognition protein 1 facilitates microtubule growth and bundling required for mitosis. Mol. Cell. Biol. *30*, 935–947.

Zhang, Y., Liu, T., Meyer, C.A., Eeckhoute, J., Johnson, D.S., Bernstein, B.E., Nusbaum, C., Myers, R.M., Brown, M., Li, W., and Liu, X.S. (2008). Model-based analysis of ChIP-Seq (MACS). Genome Biol. *9*, R137.

Zhou, Y., and Wang, T.S. (2004). A coordinated temporal interplay of nucleosome reorganization factor, sister chromatin cohesion factor, and DNA polymerase alpha facilitates DNA replication. Mol. Cell. Biol. *24*, 9568–9579.